Photo-Induced Destruction of Giant Vesicles in Methylene Blue Solutions

Wilker Caetano,*,† Paula S. Haddad,† Rosangela Itri,‡ Divinomar Severino,§ Vinicius C. Vieira,§ Mauricio S. Baptista,§ André P. Schröder,† and Carlos M. Marques†

Institut Charles Sadron, UP22 CNRS ULP, 67083 Strasbourg Cedex, France, and Instituto de Física, Universidade de São Paulo, CP 66318, and Instituto de Química, Universidade de São Paulo, 05315-970 São Paulo, SP, Brazil

Received May 27, 2006. In Final Form: September 29, 2006

We study the photodecomposition of phospholipid bilayers in aqueous solutions of methylene blue. Observation of giant unilamellar vesicles under an optical microscope reveals a consistent pattern of membrane disruption as a function of methylene blue concentration and photon density for different substrates supporting the vesicles.

Introduction

Photosensitization is the basis of photodynamic therapy (PDT), a technique that has been used to treat various solid tumors in the skin, breast, lung, bladder, and esophagus.[1−3] The method relies on the administration of a sensitizer molecule that is suitable to induce the formation of singlet oxygen ($^1O_2$) when exposed to light of the appropriate wavelength. Singlet oxygen ($^1O_2$) mediated reactions in the cell membrane eventually lead to severe tissue damage since this species is a powerful oxidizing agent, able to induce necrosis or apoptosis in cancer cells.[1−5]

Existing clinical protocols rely on a derivative of hematoporphyrin,[6−8] and intense research in this area is dedicated to the study of several variants of this family but also of many other photoactive molecules. Among these, methylene blue (MB) stands as an interesting candidate for improving the technique.[9−11] As other chromophores, it has interesting photochemical characteristics including a high quantum yield (ϕ_ρ) of singlet oxygen ($\phi_\rho \approx 0.5$) and the possibility to generate several radical species.[12−14] It also has affinity to melanin and actively binds to mitochondria,[15] a particularly interesting feature since mitochondrion destruction leads to cell apoptosis, the preferred pathway for tissue destruction that minimizes the inflammatory response.[6]

It has been determined that damaging the membranes is the key step toward cell killing.[5] Photosensitizers in general, and MB in particular, are known to promote peroxidation of unsaturated phospholipids, while no effect has been reported for saturated lipids.[16] At the molecular level, the well-known mechanism of peroxidation leads to a modification of the structural characteristics of the phospholipids including breaking of the lipid chain and formation of ketones, aldehydes, and carboxylic acids.[17] Despite extensive spectroscopy work on the chemistry of phospholipid peroxidation,[18] little is known of the deep repercussions that such molecular modifications have on the membrane cohesion and structure at the optical length scales in the 1−100 μm range, where the shape, adhesiveness, and fluctuations of the membrane can be continuously monitored under an optical microscope.

The present study is concerned with the photosensitizing effects of MB on giant unilamellar vesicles (GUVs) made from DOPC (1,2-dioleoyl-*sn*-glycero-3-phosphocholine) phospholipid membranes. We determine in this study the conditions for membrane damage of giant vesicles immersed in MB solutions and show the typical scenarios eventually leading to membrane photodestruction. Our findings contribute to a more comprehensive picture of the pathways leading to the disruption of phospholipid membranes, thus bringing new physical information into the field of photodynamic therapy.

Materials and Methods

Methylene Blue and Nonanoic Acid Solutions. MB was purchased from Sigma-Aldrich, and stock solutions were prepared in ultrapure Milli-Q water without further purification. The final MB concentration in the different solutions was checked using a spectrophotometer (Hitachi F-4010). Nonanoic acid (Aldrich, 96%)

* To whom correspondence should be addressed. E-mail: wilker@fct.unesp.br. Fax: + 55 (18) 3221-5682.

† Institut Charles Sadron.

‡ Instituto de Física, Universidade de São Paulo.

§ Instituto de Química, Universidade de São Paulo.

(1) Henderson, B. W.; Dougherty, T. J. *Photochem. Photobiol.* **1992**, *55*, 145−157.

(2) Schuitmaker, J. J.; Bass, P.; Van, Leengoed, L. L. M.; Van der Meulen, F. W.; Star, W. M.; Van Zandwijk, N. *J. Photochem. Photobiol., B* **1996**, *34*, 3−12.

(3) Jori, G.; Reddi, E. In *Photodynamic therapy of Neoplastic Disease*; Kessel, D., Ed.; CRC: Boston, 1990; Vol. 2, p 117.

(4) Foote, C. S. *Science* **1968**, *162*, 963.

(5) Valenzeno, D. P. *Photochem. Photobiol.* **1987**, *46*, 147−160.

(6) Kessel D. In *Photodynamic Therapy of Neoplastic Disease*; Kessel, D., Ed.; CRC: Boston, 1990; Vols. 1 and 2.

(7) Isayeva, T.; Kumar, S.; Ponnazhagan, S. *Int. J. Oncol.* **2004**, *25*, 335.

(8) Wajapeyee N.; Somasundaram K. *Curr. Opin. Mol. Ther.* **2004**, *6*, 296. Garrison J.B.; Kyprianou N. *Curr. Cancer Drug Targets* **2004**, *4*, 85.

(9) Miellish, K. J.; Cox, R. D.; Vermon, D. I.; Griffiths, J.; Brown, S. B. *Photochem. Photobiol.* **2002**, *75*, 392−397.

(10) Orth, K.; Ruck, A.; Stanescu, A.; Beger, H. G. *Lancet* **1995**, *345*, 519−520.

(11) Tardivo, J. P.; Del Giglio, A.; Paschoal, L. C. H.; Baptista, M. S. *Photomed. Laser Surg.* **2006**, *24*, 528−531.

(12) Tuite, E. M.; Kelly, J. M. *J. Photochem. Photobiol., B* **1993**, *21*, 103−124.

(13) Junqueira, H. C.; Severino, D.; Dias, L. G.; Gugliotti, M.; Baptista, M. S. *Phys. Chem. Chem. Phys.* **2002**, *4*, 2320−2328.

(14) Severino, D.; Junqueira, H. C.; Gabrielli, D. S.; Gugliotti, M.; Baptista, M. S. *Photochem. Photobiol.* **2003**, *77*, 459−468.

(15) Gabrieli, D.; Belisle, E.; Severino, D.; Kowaltowski, A. J.; Baptista, M. S. *Photochem. Photobiol.* **2004**, *79*, 227−232.

(16) Muller-Runkel, R.; Blais, J.; Grossweiner, L. I. *Photochem. Photobiol.* **1981**, *33*, 683−687.

(17) Gollnick, K. *Adv. Photochem.* **1968**, *6*, 2.

(18) Reis, A.; Domingues, M. R.M.; Amado, F. M.L.; Ferrer-Correia, A. J.V.; Domingues, P. *Biomed. Chromatogr.* **2005**, *19*, 129−137. Reis, A.; Domingues, M.R.M.; Amado, F.M.L.; Ferrer-Correia, A.J.V.; Domingues, P. *Biomed. Chromatogr.* **2006**, *20*, 109−118.

10.1021/la061510v CCC: $37.00
Published on Web 12/15/2006 PAGE EST: 7.2

was used without purification. A stock solution of 7.8 mM was prepared in chloroform.

Formation of Giant Vesicles. DOPC phospholipids from Avanti Polar Lipids were used as purchased. GUVs were prepared by the electroformation method.[19] A chloroform solution (ca. 20 μL) of DOPC at 1.0 mg/mL was spread on an indium tin oxide (ITO) covered glass and dried under vacuum for 1 h. A second identical glass plate was used to cover an incubation chamber delimited by a ring of Sigillum wax (Vitrex, Copenhagen, Denmark) and filled with a 0.1 M glucose solution prepared with ultrapure Milli-Q water. An ac voltage rising from 100 mV up to 2 V at a fixed frequency of 10 Hz was applied across the 1 mm chamber gap for 1 h.

Observation Chambers. The giant vesicles were transferred into a chamber made up of a 1.0 mm thick silicon window (CoverWell, Germany) previously sealed (silicone grease) onto a glass microscope slide and coated by a substrate. To investigate the influence of the substrate, we performed experiments with three different materials: clean glass (0.2 mm thickness, Marienfeld, Germany), polymeric surfaces (0.4 mm thickness, CoverWell, Germany), and hydrophobic glass obtained by the adsorption of a monolayer of octadecyltrichlorosilane (Sigma-Aldrich, France). The observation chambers were sealed to reduce convection effects to a minimum level. The chamber was filled with 0.1 M sucrose solution in the absence and presence of distinct MB concentrations ranging from 4 to 130 μM. The interplay between glucose and sucrose osmotically matches the inner and outer compartments of the vesicles and avoids their swelling and deswelling. Further, the small difference in density values is enough to drive the vesicles to the neighborhood of the upper surface to be observed by making use of a direct microscope. Conversely, inner sucrose and outer glucose solutions also containing MB were employed to observe the vesicles near the bottom surface, using the inverted microscope described below.

Visualization and Irradiation Procedures for GUVs. Pre- and postirradiated vesicle images were visualized by means of a Leica direct microscope (DMR model, with a 10× objective) and a Nikon inverted microscope (Eclipse TE200, with a 100× objective) and recorded using a video camera, Hamamatsu C5405-01, and a numeric camera, PixeLINK PL-A641-STA. The acquisition of images was controlled by homemade software. The illumination system of both microscopes (100 W halogen lamp) was used in the transmission mode (bright field), with low-intensity illumination, to observe the vesicles. We checked that, under these conditions, no perturbation of the vesicles in the presence of MB occurred over 1 h of observation. The illumination system of the Leica microscope was also used to promote the photochemical reactions in the sample, as explained below. In the case of the inverted Nikon microscope, transmission and reflection interference contrast microscopy (RICM[20]) modes were used. The RICM observation mode works with monochromatic light, obtained using a narrow-band-filtered illumination provided by a 100 W mercury lamp. RICM allows following the fluctuations of the GUV membrane in the vicinity of the substrate,[20] revealing the tension of the membrane and its degree of adhesion to the surface. We used two narrow-band filters: one blue and one green filter (Melles-Griot, $\lambda = 436$ and 547 nm, bandwidth 10 nm). The blue filter enabled RICM observation without vesicle perturbation, since the MB absorption around 436 nm is very small,[13] while the green filter was used to irradiate the sample as well as to observe the membrane behavior during the photoactivation of MB. For the wavelength $\lambda = 547$ nm the MB molar extinction coefficient is $\epsilon = 5.6 \times 10^3\ \mathrm{cm^{-1}\ M^{-1}}$,[13] corresponding to an MB molar absorbance cross section $\sigma = 0.1\ \text{Å}^2$. The analyzer and polarizer were not used in the RICM experiment at 547 nm[20] to retain the highest possible light intensity. The total density power in the RICM mode at 547 nm was measured by a silicon photodiode LM2 with an X1000 attenuator and coupled to a Field Master GS from Coherent and was found to be $P = 10\ \mathrm{W\ cm^{-2}}$. Keeping the green light on, we could also observe the vesicles in transmission mode with low-intensity bright field irradiation, since the green light reflected by the sample was much lower than the white light used to image the vesicle contour.

Liposome Formation and Irradiation. A 25 mg sample of DOPC phospholipids was dissolved in 3 mL of chloroform and evaporated under nitrogen, forming a thin film. After hydration of this film in Milli-Q water, we obtained a suspension of multilamellar vesicles that was transferred to a 50 mL volumetric flask, the volume of which was completed with water. The vesicle suspension was sonicated (Braunsonic 1510) for 5 min to make small unilamellar vesicles that will be referred to as liposomes. After sonication the dispersion was centrifuged at $3500 \times 9.8\ \mathrm{m\ s^{-2}}$ for 2 min to remove titanium particles. The liposomes were then added to a 55 μM MB solution. The final concentration of lipids in the mixture was 0.6 mM. Irradiation of the liposome suspensions was performed in a Petri dish with a 665 nm laser (Laser Line Inova—medial intelligent laser therapy controller). The light intensity was 100 mW, and the light beam was expanded to a surface of 9 $\mathrm{cm^2}$ over 170 min. This corresponds to a light dose of 113 J $\mathrm{cm^{-2}}$. At this wavelength $\epsilon = 8.2 \times 10^4\ \mathrm{cm^{-1}\ M^{-1}}$,[13] corresponding to an MB molar absorbance cross section $\sigma = 1.4\ \text{Å}^2$.

Surface Tension Measurements. The surface tension for various liposome suspensions was obtained using the ring method in a Du Noüy tensiometer (Fisher Scientific Tensiomat, model 21, Fisher Scientific) properly calibrated. The measurements were made by injecting 5 mL of a liposome solution, irradiated or nonirradiated, in 35 mL of Milli-Q water in a Teflon container. Successive measurements were performed over 80 min for each of the solutions. The surface tension for a solution of nonanoic acid (NA) was also obtained by spreading on the air−water interface or injecting in the water subphase 50 μL aliquots from the 7.8 mM stock solution.

Results

We performed experiments at room temperature with both giant unilamellar vesicles and liposomes. We first present results for experiments carried out on GUVs immersed in MB solutions of different concentrations. The contact between the phospholipid bilayers and the MB solution did not lead to vesicle destruction, as long as the solution was kept in the dark, or illuminated gently, as for the observation with the microscope in the transmission mode, using a low intensity. However, immersion of the vesicles in the MB solution did lead to both an increase of membrane fluctuations and a significant increase of the adhesion of the vesicles to the glass substrate. The latter might be correlated to an increase of the MB concentration in the neighborhood of the glass substrate. Indeed no vesicle adhesion was exhibited by hydrophobic fluorosilanized glasses or by polymeric substrates. The MB adsorption onto glass substrates has been previously reported[21,22] and also observed in our experiments. As we will see below, this might influence the destruction scenario for the vesicles, but it does not lead by itself to the bilayer disruption.

Observation of Giant Vesicle Behavior under White Light. Giant vesicles immersed in MB solutions were first observed in a bright field using the Leica microscope. Observation of the vesicles for 15 min under normal illumination conditions did not lead to any noticeable perturbation of the vesicle behavior. The sample was then overexposed to the halogen lamp irradiation by totally opening the microscope diaphragm and by increasing the lamp power to its maximum. A complete experiment cycle comprised then (i) a 15 min initial observation followed first by (ii) 1 min of irradiation and 1 min of observation and then by (iii) the repetition of an irradiation/observation sequence up to five times and by (iv) a final observation of 15 min during which

(19) Angelova, M.; Imitrow, D. *Mol. Cryst. Liq. Cryst.* **1987**, *152*, 89.
(20) Rädler, J.; Sackmann, E. *J. Phys II* **1993**, *3*, 727−748.
(21) Ohline, S. M.; Lee, S.; Williams, S.; Chang, C. *Chem. Phys. Lett.* **2001**, *346*, 9−15.
(22) Kobayashi, H.; Takahashi, M.; Kotani, M. *Chem. Phys. Lett.* **2001**, *346*, 376−382.

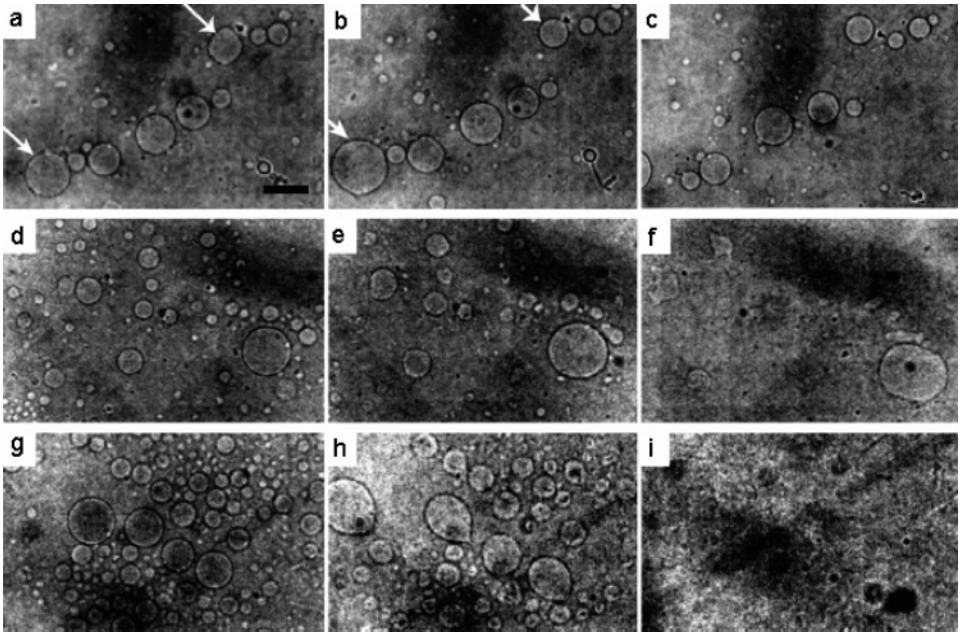

Figure 1. Effect of exposure to light of giant vesicles immersed in MB solutions. The bar size is 50 μm. For MB concentrations below 10 μM no effect can be detected. (a)−(c) show giant vesicles in a 10 μM MB solution. At this concentration, only a slight disturbance of the vesicle contour is detected after the first irradiation. Further illumination does not produce any visible effect. (d)−(f) show vesicles in a 25 μM MB solution: (d) no irradiation, (e) after 1 min of irradiation, (f) after 3 min of irradiation. All vesicles are destroyed after 4 min. (g)−(i) show vesicles in a 55 μM MB solution: (g) no irradiation, (h) 1 min of irradiation, (i) 2 min of irradiation.

no further effects were detected. Images discussed below were taken during the observation sequences. The total time of an experiment was then 40 min. A precise measure of the light power density of the white light reaching the sample was not attempted, given the wide spectrum characteristics of the halogen lamp. A quantitative study of the relationship between photon flux and membrane destruction will be presented below in the paragraph describing single vesicle behavior under green-light illumination.

Parts a−c of Figure 1 show a typical irradiation experiment for vesicles exposed to an MB concentration of 10 μM at room temperature. Experiments performed at concentrations below 10 μM did not reveal any influence of the light on the vesicle morphology or fluctuation behavior. At 10 μM some modifications of the vesicle behavior, indicated by the arrows in Figure 1a,b, were observed after 1 min of irradiation. Figure 1a shows the giant vesicle sample before the first irradiation, whereas Figure 1b displays a mild deformation of the vesicle shapes after the first exposure to the maximum photon density. The main discernible effect is a slight fluctuation of the vesicle contours that deviate from their initial shapes. However, after a second exposure to a high photon density, the vesicles quickly stabilize their shapes and remain after that insensitive to further irradiation, as shown in Figure 1c.

A significant impact of the illumination can be seen for an MB concentration of 25 μM. As usual, the preliminary observation of the vesicles under a low light intensity did not reveal any changes (Figure 1d). Nevertheless, the cumulative effect of exposure to a maximum intensity beam eventually destroys the GUVs. As an example, parts e and f of Figure 1 display the evolution of the vesicle morphology to increasing doses of photons corresponding to 1−4 min of illumination. As the figures show, the size and shape of the vesicles are already modified after the first minute of irradiation (Figure 1e). A strong deformation and destruction of the smaller vesicles follows after the third minute of irradiation (Figure 1f). Vesicles of all visible sizes were completely destroyed after an irradiation time of 4 min.

Stronger and faster effects were observed at two higher MB concentrations of 55 and 130 μM. Parts g−i of Figure 1 present images for vesicles observed under these conditions. They show evidence for a strong perturbation of the size and the shape of the larger vesicles after 1 min only of high-intensity illumination (Figure 1h). This perturbation is concomitant with the destruction of the smaller vesicles in the sample. All vesicles were destroyed after 2 min of exposure to the beam (Figure 1i).

Given the known photochemistry characteristics of MB, the observed effects are to be directly correlated to the generation of $^1O_2$. However, MB and other sensitizers also generate heat that may cause a relatively large local temperature increase in the membrane microenvironment that could in principle affect the membrane. To make sure that the observed effects were due to $^1O_2$, sodium azide, a known singlet oxygen suppressor,[5] was added to a vesicle solution at a concentration of 5 mM in the presence of 55 μM MB. Under these conditions, we observed that a 4 times larger illumination was required to induce vesicle destruction, thus confirming the role of $^1O_2$ in the photodesctruction of the phospholipid vesicles. Moreover, no vesicle destruction was observed by heating the sample to 40 °C in the absence of strong illumination. Both results give support to conclude that $^1O_2$ generation is the main factor leading to the vesicle damage.

There is a clear interrelation between the MB concentration and the irradiation time needed to cause photoinduced damage to the GUVs under polychromatic light, in such a way that a shorter period of irradiation time is enough to destroy vesicles dispersed in solutions of higher amounts of MB. However, we also found, within our experimental protocol, that MB concentrations equal to or larger than a 25 μM threshold are required to induce noticeable damage of the membranes. Having at this point determined the MB concentrations necessary to destroy the giant vesicles, we now turn to a detailed description of the pathways leading the giant vesicles through a series of transformations. We proceed by studying single-vesicle behavior under a monochromatic green light.

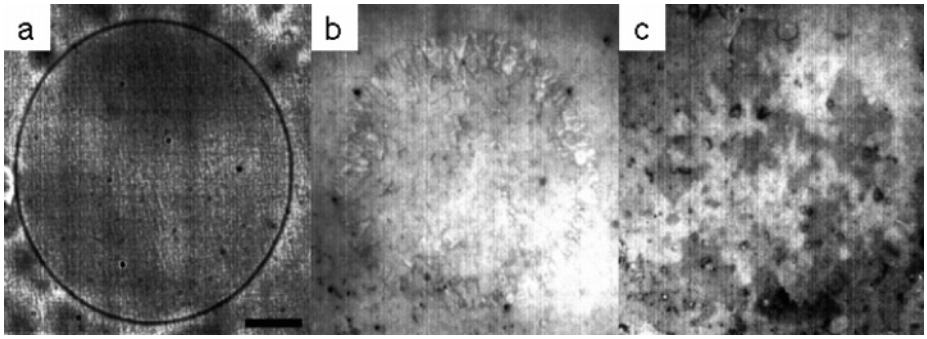

Figure 2. (a) Transmission optical microscopy image of a giant vesicle in 55 μM MB solution, close to the glass substrate. The bar size is 10 μm. (b) RICM image of the contact zone between the vesicle and the substrate. Uniformity in the gray levels indicates strong adhesion and absence of fluctuations. (c) The membrane has been destroyed by irradiation. The surface retains fragments of the destroyed membrane.

Individual Vesicle Behavior under Green Light. To directly observe the behavior of the vesicles exposed to a light source of a narrow wavelength range, we used a combination of filters in the inverse Nikon microscope. This allowed observation of the vesicles at a high magnification of a 100× objective in the RICM mode. As with the Leica microscope, we also used the transmission mode under low illumination conditions. Thus, information on both the shape of the vesicles at the level of their equators and the interaction region between the vesicle and the substrate[20] could be obtained. In the RICM mode the light source from the mercury lamp was shifted, after some initial observation time under blue filtered light, to the green wavelength to provide a suitable light source for MB excitation and concurrent vesicle observation. Destruction of the vesicles was performed under a light power of 10 W cm^{-2}. Reported irradiation times start at the beginning of exposure to the green light.

To keep the total observation time of vesicle destruction below 15 min, we chose to work at MB concentrations above the crossover concentration of 25 μM. Results shown below have been obtained in 55 and 130 μM solutions of MB.

When the interactions between the vesicle and the substrate lead to a strong adhesion pattern, detected by a typical homogeneous gray patch exhibited in the RICM images, the irradiation induces the vesicle destruction on the substrate. This is shown in the sequence of images in Figure 2. Figure 2a shows a typical transmission image of a giant vesicle of 40 μm. In Figure 2b, the corresponding RICM image displays the contact zone between the vesicle and the glass substrate. The internal part of the adhesion zone does not exhibit dynamic fluctuations of its gray levels. The diameter of the adhesion circle is 38 μm, comparable to the diameter of the transmission image, indicating an almost hemispherical shape of the adhered GUV. Under illumination, the vesicle increases its adhesion to the substrate, as seen by the increase of both its transmission and the RICM diameters, not shown. After roughly 1 min of exposure to the green light, corresponding to a light dose of 600 J cm^{-2}, the vesicle is destroyed and collapses on the substrate. Evidence for destruction of the vesicle comes both from the absence of a transmission image and from the chaotic increase of the adhesion pattern shown in Figure 2c. Indeed, the image displays the central adhered region but also peripheral fragments adsorbed consecutively to the vesicle collapse.

In the case where the adhesion of the vesicle to the substrate is weak, the destruction of the vesicle occurs in the bulk following a first desorption mechanism that we now describe. Figure 3 shows a series of snapshots for a GUV that displayed initially large shape fluctuations—see Figure 3a—as well as a weak adhesion patch evidenced by the fluctuating pattern in Figure 3b. Under illumination, the contact area between the vesicle and the substrate first increases in size: this suggests that the tension on the membrane is first released. The presence of a fluctuating pattern indicates, however, that there is no increase of adhesiveness between the membrane and the glass. The subsequent images in Figure 3c−e show the reduction of the vesicle contact zone, further supporting the absence of a strong adhesion to the surface. This size reduction is due to an increase in vesicle tension, shown by the circularity of the interference rings in Figure 3e and by the circular shape of the final transmission image in Figure 3f.

After the sequence of events shown in Figure 3, the vesicle left the surface and was eventually destroyed in the bulk. We describe now the typical transformations of the vesicle shape that lead to complete destruction of the vesicles. Under continuous irradiation, there are two distinct scenarios for vesicle destruction, yielding the same final structure for the remaining material. In the first one, shown in parts a−c of Figure 4, which displays the bulk evolution of the vesicle already seen in Figure 3, minute lenses start to nucleate on the membrane surface after ca. 4 min of irradiation, or 2400 J cm^{-2}. These lenticules must contain new molecules resulting from reactions mediated by singlet oxygen produced by MB light absorption. As further discussed below, we believe that these comprise photooxidized products of lipids. Two main features can be observed: (i) a continuous decrease in size of the spherical vesicle, as shown in Figure 4b, roughly at a rate of 5 μm/min, and (ii) an increase of the number of lenticules and an occasional increase of their sizes by coalescence of two smaller lenses. Events related to these phenomena can be observed in Figure 4b where pictures from several vesicles are displayed. The final state of the vesicle is a droplet displayed in Figure 4c that is totally blue as visualized in the microscope ocular. In the second event, the nonadhered GUV, shown in Figure 5a, suffers a dramatic rupture of the membrane, displayed in Figure 5b, within 1−3 min of irradiation without the appearance of small lenses. After the initial stage, it forms a kind of aggregate composed of small fragments of the former membrane (not shown) that also evolves to a blue droplet as revealed in Figure 5c.

Finally, for the largest MB concentration, we observed similar behaviors, whatever the nature of the substrate, i.e., glass or polymer. Typically, under illumination a nonadhered vesicle moves toward the surface where it strongly adheres and then collapses. Occasionally, during the vesicle collapse, fragments of the membrane escape to the bulk and evolve into a final blue droplet, similarly to the other cases.

Discussion

This work focused on the modifications experienced by DOPC bilayers exposed to singlet oxygen, a reactive species generated

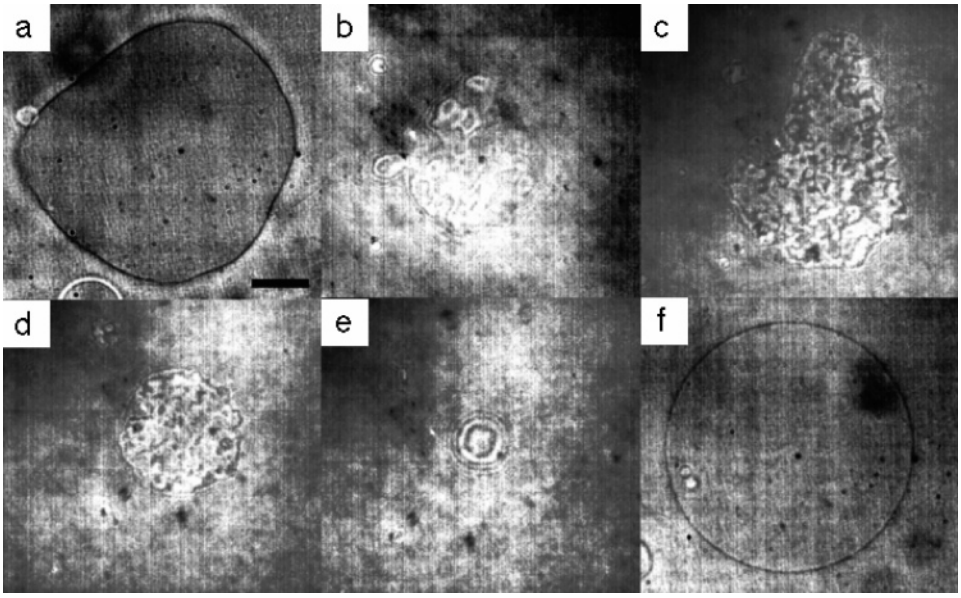

Figure 3. (a) Transmission optical microscopy image of a very floppy giant vesicle in a 55 μM MB solution, close to the fluorosilanized substrate. The bar size is 10 μm. (b) RICM image showing surface fluctuations, indicative of small adhesion. (c)−(e) After irradiation the vesicle tension grows and eventually detaches from the surface, leading to a (f) tense vesicle in the bulk. The vesicle is later destroyed in the bulk.

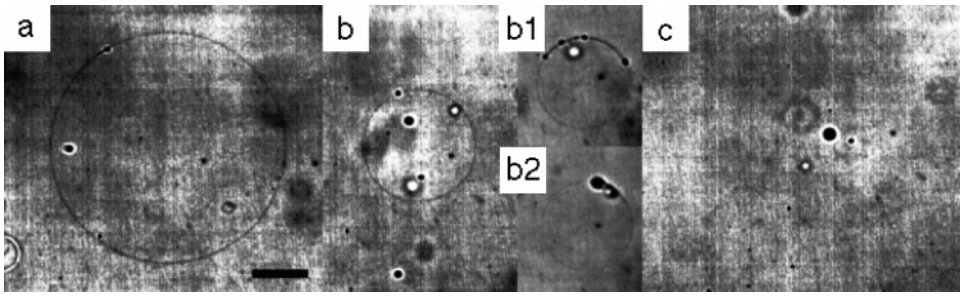

Figure 4. (a) Transmission optical microscopy image of the vesicle already shown in Figure 3. After leaving the surface, the vesicle starts to shrink at roughly a rate of 5 μm/min, while small blue lenticules spontaneously appear on the membrane. The bar size is 10 μm. (b) During shrinkage more lenticules (b1) appear, while some of them (b2) merge to make large ones. (c) At the end of the process only a blue bead remains in the solution, certainly containing photooxidized products of lipids and a significant amount of methylene blue.

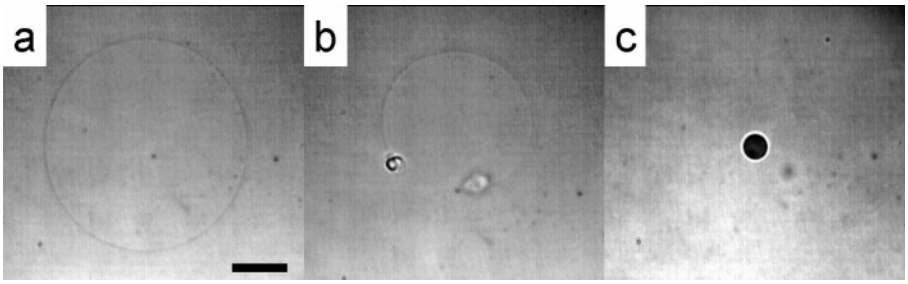

Figure 5. A different evolution scenario for a bulk vesicle in a 55 μM MB solution. The bar size is 10 μm. (a) Transmission image of the original, unperturbed vesicle. (b) A sudden disruption of the membrane opens a large hole. (c) The vesicle evolves to a final state similar to the one described in Figure 4 with a blue bead collecting the products of photooxidization.

by light irradiation of MB solutions. We observed by optical microscopy the sequence of transformations eventually leading to the destruction of the phospholipid membranes immersed in various amounts of the MB photosensitizer. We followed these pathways to disruption both at low 10× magnification under a white light source and at larger 100× magnification under green light. In both cases, vesicle destruction was achieved by up to 4 min of illumination for MB concentrations larger than 25 μM, regardless of the substrate. We now summarize some of the key observations made during this work and discuss the physical and chemical events that lead to vesicle disruption.

The destruction of the vesicles is thus achieved by a green light dose of a few thousand joules per square centimeter. Furthermore, the observed reduction in the vesicle diameter of 5 μm/min indicates a phospholipid damage rate of roughly 1% per second. At the same time, a small number of lenticules

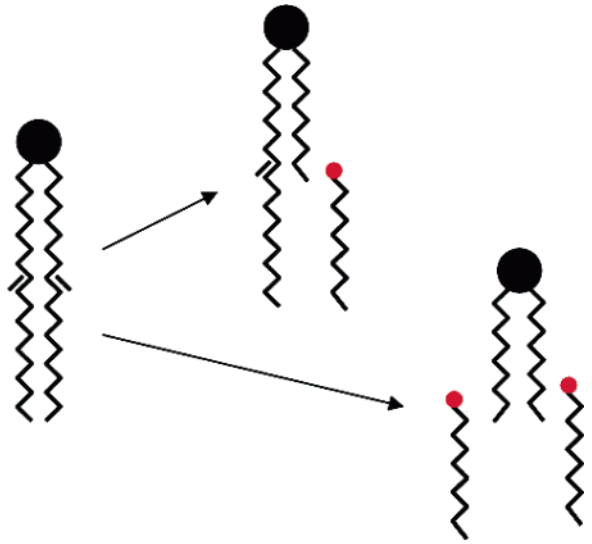

Figure 6. Schematic effect of the phospholipid photodestruction. When singlet oxygens react with the unsaturated bonds of a phospholipid molecule, the tail size is effectively reduced, generating a number of surfactant-like fragments.

nucleates on the vesicle membranes. These microscopic membrane bulges suggest that at least some of molecules resulting from phospholipid damage are collected within the bilayers.

Carbon−carbon double bonds in lipid chains are known to be labile to peroxidation by singlet oxygen ($^1O_2$), a chemical reaction mechanism that destabilizes membranes, inducing their lysis.[24] In the present experiments, $^1O_2$ might be produced both in the membrane and in the surrounding solution. Although one might be tempted to attribute a particular role to the MB molecules present in the membrane, we will see below that oxygen singlet species are collected at the membrane surface from the nearby solution, over a thickness of 100 nm. The amount of these species is much larger than the number of $^1O_2$ species generated in the membrane for any realistic MB partition coefficient.[23]

Thus, we can consider that $^1O_2$ is only generated in the surrounding solution, and we have to estimate the amount of $^1O_2$ that reaches the membrane per unit time and unit surface. The maximum flux of $^1O_2$ reaching the membrane surface can be obtained by solving a diffusion equation for the space and time evolution of the $^1O_2$ concentration $C(z,t)$: $\partial C/\partial t = D(\partial^2 C/\partial z^2) - C/\tau + Q$, where z is the space coordinate perpendicular to the surface, D is the diffusion coefficient of singlet oxygen, $D = 3 \times 10^{-5}$ cm^2 s^{-1} in water,[25] τ is the decay time of $^1O_2$, $\tau = 3 \times 10^{-6}$ s in water,[26] and Q is the number of singlet oxygen species generated by unit time and unit volume. Given a molar absorbance cross section σ of MB in water, the $^1O_2$ production rate can be written as $Q = (\phi_\rho[\mathrm{MB}]\lambda P\sigma)/(hc)$,[27] with [MB] the molar MB concentration, λ the light wavelength, P the light power density, h the Planck constant, c the speed of light, and $\phi_\rho = 0.5$ the quantum yield of $^1O_2$ generation in aqueous solutions. From the concentration profile $C(z,t)$ obtained from the diffusion equation with appropriate initial and boundary conditions (we assume $C(z,t{=}0) = 0$ and $C(z{=}0,t) = 0$), one gets the flux $J = D(\partial C/\partial z|_{z=0}) = Q\delta$, where $\delta^2 = D\tau$. For our conditions, at a molar MB concentration of 55 μM, one gets a diffusion length $\delta = 100$ nm and a flux $J = 5 \times 10^{-3}$ singlet oxygen molecules Å^{-2} s^{-1} for the green light where $\sigma = 0.1$ Å.^{2} Then an area of the membrane of 50 Å,^{2} equivalent to the area occupied by a phospholipid molecule, is exposed on average to a new $^1O_2$ molecule every 4 s. In this area there are two double bonds, one for each of the two chains belonging to the phospholipid. Each of these two double bonds can potentially react with the incoming singlet oxygen species. The efficiency for such a reaction can be estimated from the observed degradation rate of the phospholipid membranes. Under our observation conditions we measure a vesicle surface reduction of 1% per second. Assuming that when the vesicle is destroyed, i.e., after 100 s, each phospholipid has lost one of its chains, we deduce that such a reaction event occurs on average in 50 Å^2 every 100 s. Breaking one unsaturated bond requires thus on average 25 singlet oxygen species; we conclude that 4% of the $^1O_2$ molecules reaching the surface are efficient in cutting the chains. If the lysis of both chains of each lipid is necessary to promote the membrane damage, then the efficiency would increase by a factor of 2.

The DOPC molecules used in this study have a double bond between the ninth and the tenth carbon atoms along each of the 18-carbon tails. Figure 6 shows schematically two possibilities of chain cleavage resulting from the interaction between the double bond DOPC and the oxygen singlet, namely, the photolysis of one or two chains. The pathway leading to this end involves the attack of singlet oxygen to the double bond, forming allylic hydroperoxides that could lead to Hock cleavage forming shorter chain aldehyde and enol molecules that can be further oxidized to carboxylic acid.[17,18] If one chain is cut, the phospholipid becomes asymmetric and one chain with nine carbon atoms, which could be nonanoic acid, is liberated into the membrane environment or into the solution. If the two chains are sliced, the phospholipid is transformed into a symmetric shorter molecule and two nine-carbon chain amphiphilic molecules are generated. Since the critical micellar concentration (cmc) of these shorter amphiphilic molecules is much higher than the cmc of the DOPC, we expect that the shorter chains can be easily ejected into the solution.

To check for the formation of short carbon chains, due to photolysis induced by the singlet oxygen, surface tension measurements were performed on solutions containing DOPC liposomes in 55 μM MB. We measured (i) nonirradiated liposome solutions, (ii) liposome solutions irradiated under red light ($\lambda =$ 665 nm) with a dose of 113 J cm^{-2}, and (iii) different concentrations of nonanoic acid. Results are presented in Figures 7 and 8. From Figure 7, it is clear that DOPC vesicles do not modify the surface tension of the air−water interface. Therefore, we can assume that in the absence of MB no phospholipid is transferred from the nonirradiated liposomes to the air−water surface. In MB solutions of nonirradiated liposomes there is a finite decrease of the surface tension, which is probably due to the MB-assisted transfer of phospholipids from vesicles to the surface. It has been determined before that MB can stabilize surface-active agents at the air−water interface.[13] It is worth stressing that a 55 μM MB in aqueous solution has, within experimental error, the same interface tension as pure water. A

(23) The amount of MB bound to the membrane can be estimated from known values for the partition coefficient of MB in the 1-octanol/water system. It has been shown for this system (Engelmann, F. M.; Rocha, S. V. O.; Toma, H. E.; Araki, K.; Baptista, M. S. *Int. J. Pharm.*, in press) that the partition coefficient (log P_{OW}) of MB is 0.4. The molar ratio of MB between the oil and water phases is therefore close to 2.5 under the condition that the oil and aqueous phases are at the same molar fraction. For a molar ratio of oil to water similar to the lipid water ratio under our experimental conditions, $\sim 10^{-4}$, there is a negligible amount of MB bound to the membranes: 0.03 μM at the highest MB concentration used of 130 μM.

(24) Anderson, V. C.; Thompson, D. H. *Biochim. Biophys. Acta* **1992**, *1109*, 33−42.

(25) Linding, B. A.; Rodgers, M. A. *J. Photochem. Photobiol.* **1981**, *33*, 627−634.

(26) Rodgers, M. A. J.; Snowden, P. T. *J. Am. Chem. Soc.* **1982**, *104*, 5541−5543.

(27) Busch, N. A.; Yarmush, M. L.; Toner, M. *Biophys. J.* **1998**, *75*, 2956−2970.

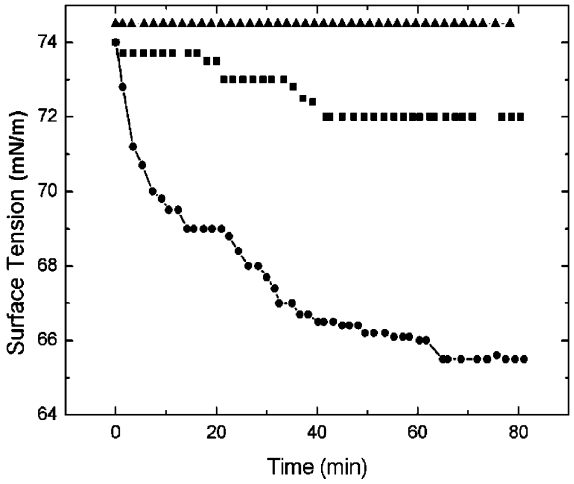

Figure 7. Surface tension of a liposome solution as a function of time: (▲) no MB, (■) in the presence of 55 μM MB, without illumination, (●) in the presence of 55 μM MB, after 170 min of continuous illumination under red light (113 J cm^{-2}, $\lambda = 665$ nm).

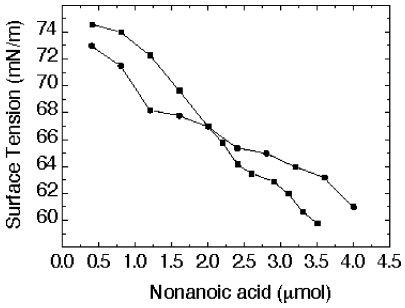

Figure 8. Surface tension of nonanoic acid solutions: (■) for deposition at the air−water interface, (●) for direct dilution in the solution.

large effect is observed in irradiated MB solutions containing liposomes. In this case the surface tension is reduced to values as low as 65 mN·m^{-1}, an effect that must be due to the transfer of photolysis amphiphilic products to the interface.

Differently from phospholipids, nonanoic acid quickly migrates to the aqueous−air interface, independently of the preparation procedure, decreasing the surface tension (Figure 8). Note that the decrease in surface tension observed for ~2.5 μM nonanoic acid is similar to the value obtained for the decrease in surface tension in the irradiated vesicle suspension ($\gamma = \sim 7$ mN/m). Assuming that at least one DOPC alkyl chain is broken during photolysis, we would generate 3.2 μM amphiphilic products, which is in good agreement with the observed decrease in surface tension caused by 2.5 μM nonanoic acid. Although a quantitative comparison between tension results from the nonanoic acid and the degraded liposome solutions is precluded by the fact that different amphiphilic molecules are generated during photolysis,[18] this experiment qualitatively shows that the photolysis of DOPC vesicles generates surface-active agents that reduce the surface tension at the water−air interface.

Another important visible effect of the membrane degradation is the formation of lenticules that can first be seen after roughly 2 min of illumination and then grow either as independent objects, presumably by collecting the reaction products, or by fusion events between two different lenticules. These lenticules are blue and eventually become very large, remaining in solution after all the membranes have been consumed. We speculate that these lenticules are formed by a mixture of short amphiphilic molecules from the photoreaction and MB. MB and negatively charged amphiphilic molecules form strong complexes[13,14] and may stabilize an inner compartment of lens shape, containing the more hydrophobic products of the reaction. Theoretical scenarios for segregation of the reaction products in the plane of the membrane and eventual destruction of the bilayer have been proposed in the literature,[27] without considering however the formation of lenticules.

Conclusions

Despite extensive past studies on phospholipid peroxidation, within the context both of photodynamical therapy and of more fundamental studies, very little is known about the consequences at the micrometer level of lipid degradation on the architecture of fluid membranes, which are structurally of prime importance in living systems. The present work is an effort to bridge the existing wide gap between the angstrom length scales where known chemical reactions take place and the micrometer dimensions of self-assembled phospholipid membranes. Our results revealed in particular what impact the well-known microscopic mechanisms of singlet oxygen induced peroxidation have on the structure of the self-assembled phospholipid bilayers. Whereas the large majority of previous work in this area concerned bulk spectroscopic techniques (fluorescence, EPR, Raman), the structural information that we provided was obtained from the observation of single individual objects, giant vesicles which contain roughly a few hundred million phospholipid molecules or 1 fmol.

Observation by optical microscopy of the modifications induced on giant vesicles by illuminating the methylene blue solution where they were suspended revealed the cascade of events that ultimately leads to the vesicle destruction. A coherent picture emerged from our observations that we now summarize.

At the source of the membrane disruption is the generation of singlet oxygen species by the methylene blue molecules present everywhere in the solution. Given the physical properties of singlet oxygen, a short-lived species with a fast diffusion coefficient, we can picture each giant vesicle as being aureoled by a corona of roughly 100 nm from where active destructive species can originate. This aureole is responsible for a singlet oxygen flux that degrades a phospholipid molecule with efficiency on the order of one chain scission per 25 $^1O_2$ molecules reaching the membrane surface.

The degradation of the membrane, observed under an optical microscope, follows a consistent pathway, and its kinetics is mainly governed by the frequency at which the chain scissions occur. At MB concentrations below 25 μM the rate of phospholipid degradation is too small to induce any noticeable changes during the time of the experiment that may last a few hours. For concentrations above 25 μM a progressive modification of the vesicle is observed that results in the reduction of its size with a concomitant formation of blue-colored lenticules. The size reduction is due to the ejection from the membrane of soluble peroxidation products. The lenticules, formed by the association of hydrophobic reaction products and MB, eventually grow into large blue droplets that are the only visible bulk objects remaining after completion of the vesicle destruction. When the MB concentration is very large, typically above 100 μM, the destruction of the vesicle follows an abrupt pathway, with the formation of large pores in a nearly explosive manner.

When the vesicle is close to an adhesive surface, the destruction can be assisted by the surface interactions, the final fate of the

(28) Wentworth, P., Jr.; et al. *Science* **2002**, *298*, 2195.
(29) Poon H.F., Calabrese V., Scapagnini G., Butterfield D.A. *Clin. Geriatr. Med.* **2004**, *20*, 329. Briganti S., Picardo. M. *J. Eur. Acad. Dermatol. Venereol.* **2003**, *17*, 663−669.

membrane being in this case shared between an irregular patchwork of bilayer chunks spread on the surface and blue droplets ejected into the bulk.

We hope that our observations will inspire future work for further exploration of the effects of photoactive reactive species within phospholipid membranes, comparing for instance phospholipids with different degrees and positions of the unsaturated bonds or phospholipids with different head groups. This might help to eventually explain the complex and unresolved aspects of phenomena related to photoinduced biomembrane damage.[28] Finally, let us also recall that membrane disruption is not only important in PDT. It is also important in several diseases such as inflammation, cancer, Parkinson's, Alzheimer's, and arthrosclerosis:[29] other areas of biology and medicine would certainly benefit from more input on the structural membrane changes that occur at the micrometer length scales.

Acknowledgment. We are grateful to CNPq/CNRS (Joint Project No. 16523) for support. We also thank Dr. M. H. G. Medeiros (Instituto de Química, Universidade de São Paulo) for helpful discussions.

LA061510V